Journal of Hyperstructures 3 *(1) (2014), 53-67.*
ISSN: 2251-8436 print/2322-1666 online

PROPORTIONAL FACTORS ESTIMATION IN AN IHCP

MORTEZA GARSHASBI AND HATEF DASTOUR

Abstract. In this paper, a numerical scheme is developed based on mollification method and space marching scheme for solving an inverse heat conduction problem. The proposed inverse problem contains the estimation of two unknown functions at the boundaries named proportional factors. The temperature and heat flux measurements in an interior point are considered as overspecified data with the presence of noise. Convergence and stability of the solution for the proposed method are analyzed. To support the numerical achievements, some numerical examples are considered and discussed.

Key Words: Inverse heat conduction problem, marching scheme, mollification method.
2010 Mathematics Subject Classification: Primary: 80A23; Secondary: 65F22, 65M12.

1. Introduction

When a flat plate is cooled from an initial uniform temperature by a fluid at another temperature, the temperature distribution, which varies with time, can be described by the transient heat conduction solution. Generally when the transfer of heat from liquids to solids is considered, the heat flux is often taken to be proportional to the difference in the boundary temperature of the solid and the temperature of the liquid. The convection can provide a possible boundary condition for conduction problems in the form of a heat transfer coefficients. In dealing with heat transfer by convection, i.e. energy transport between fluids and surfaces, we are mainly concerned with determination of unknown

Received: 10 April 2014, Accepted: 5 June 2014. Communicated by D. Khojasteh Salkuyeh;
∗Address correspondence to Morteza Garshasbi; E-mail: m_garshasbi@iust.ac.ir

parameters for various systems and investigating how the heat transfer coefficient varies as a function of the fluids properties, such as thermal conductivity, viscosity, density and specific heat, the system geometry, the flow velocity and the temperature differences [14].

The identification of coefficients in parabolic equations named inverse heat conduction problems (IHCPs) usually are ill-posed problems that have received considerable attention from many researchers in a variety of fields, using different methods [2, 4, 9]. The IHCPs arise in the modeling and control of processes with heat propagation in thermophysics and mechanics of continuous media. Inverse problems are in nature unstable because the unknown solutions and parameters have to be determined from indirect observable data which contain measurement error. The major difficulty in establishing any numerical algorithm for approximating the solution is due to the severe ill-posedness of the problem and the ill-conditioning of the resultant discretized matrix. The studies of inverse heat conduction problems are even more difficult. Although heat conduction process is very smooth, the process is irreducible. This means that the characteristic of the solution (for instance, the shape of the interior heat flow) may not be affected by the observed data. Some detailed treatments of problems in these areas can be found in [1, 5, 8, 11, 13, 15].

In this paper, the framework is a one dimensional nonlinear heat conduction model and our problem is to identify two time dependent coefficients in the boundary conditions of the proposed problem. Our strategy is to obtain a numerical scheme for the approximation of the unknown functions by implementing a combination of discrete mollification and a space-marching finite difference numerical scheme. The regularization tool is the mollification method, which is a reliable regularization procedure that has been widely applied for the stable numerical solution of ill-posed problems based on parabolic equations [12, 11, 13, 10].

The remainder of the paper is organized as follows: In Section 2 we review basic facts about the discrete mollification operator. Section 3 is devoted to the identification problems. Section 4 includes the stability and convergence analysis of the proposed numerical method. Finally in section 5 two illustrative numerical examples are investigated.

2. Problem description

2.1. **Inverse problem formulation.** Consider the transfer of heat from liquids to solids is occurred. As mentioned before, the heat flux is often taken to be proportional to the difference in the boundary temperature of the solid and the temperature of the liquid. The mathematical model of this phenomenon, in the one dimensional space, may be considered as follows [3]

$$u_t(x,t) - a^2 u_{xx}(x,t) = f(x,t), \qquad 0 < x < 1,\ 0 < t < 1, \tag{2.1}$$

$$u(x,0) = \gamma(x), \qquad 0 \le x \le 1, \tag{2.2}$$

$$u_x(0,t) + \zeta(t)u(0,t) = g(t), \qquad 0 \le t \le 1, \tag{2.3}$$

$$u_x(1,t) + \eta(t)u(1,t) = h(t), \qquad 0 \le t \le 1, \tag{2.4}$$

where $f(x,t)$ and $\gamma(x)$ are considered to be a known bounded functions and $\zeta(t)$ and $\eta(t)$ are known as proportional factors. Identification of these coefficients is the goal of this work. For this end one my needs some overspecified data. Here we consider that the temperature and heat flux at an interior point such as x^* is at hand. With this assumption, the following auxiliary problem is considered

$$u_t(x,t) - a^2 u_{xx}(x,t) = f(x,t), \qquad 0 < x < 1,\ 0 < t < 1, \tag{2.5}$$

$$u(x,0) = \gamma(x), \qquad 0 \le x \le 1, \tag{2.6}$$

$$u(x^*,t) = \varphi_1(t), \qquad 0 \le t \le 1, \tag{2.7}$$

$$u_x(x^*,t) = \varphi_2(t), \qquad 0 \le t \le 1. \tag{2.8}$$

By solving this problem and determining the functions $u(x,t)$ and $u_x(x,t)$ one may find the unknown functions $\zeta(t)$ and $\eta(t)$.

In the sequel a numerical marching scheme based on mollification method will be introduced to find the solution of the problem (2.5)-(2.8) under the assumption that $\varphi_1(t)$, $\varphi_2(t)$, $g(t)$ and $h(t)$ are only known approximately as $\varphi_1^\varepsilon(t)$, $\varphi_2^\varepsilon(t)$, $g^\varepsilon(t)$ and $h^\varepsilon(t)$ such that

$$\|\varphi_1(t) - \varphi_1^\varepsilon(t)\|_\infty \le \varepsilon, \tag{2.9}$$

$$\|\varphi_2(t) - \varphi_2^\varepsilon(t)\|_\infty \le \varepsilon, \tag{2.10}$$

$$\|g(t) - g^\varepsilon(t)\|_\infty \le \varepsilon, \tag{2.11}$$

$$\|h(t) - h^\varepsilon(t)\|_\infty \le \varepsilon. \tag{2.12}$$

Because of the presence of the noise in the problem's data, we first stabilize the problem using the mollification method [11, 12].

2.2. **Regularized problem and the marching scheme.** To solve the problem (2.5)-(2.8), first it reduces to determining $v(x,t), v_x(x,t) \in$

$[0,1]\times[0.1]$ while they are satisfying following conditions

$$v_t(x,t)-a^2u_{xx}(x,t)=f(x,t),\qquad 0<x<1,\ 0<t<1, \tag{2.13}$$

$$v(x,0)=J_{\delta_i'}\gamma(x),\qquad 0\le x\le 1, \tag{2.14}$$

$$v(x^*,t)=J_{\delta_0}\varphi_1(t),\qquad 0\le t\le 1, \tag{2.15}$$

$$v_x(x^*,t)=J_{\delta_0^*}\varphi_2(t),\qquad 0\le t\le 1, \tag{2.16}$$

where the radii of mollification, δ_0, δ_0^* and δ' are chosen automatically using the generalized cross validation (GCV) method [11]. Then $Zeta(t)$ and $Eta(t)$ (mollified versions of $\zeta(t)$ and $\eta(t)$) from the following equations.

$$v_x(0,t)+Zeta(t)v(0,t)=J_{\delta_0''}g(t),\qquad 0\le t\le 1, \tag{2.17}$$

$$v_x(1,t)+Eta(t)v(1,t)=J_{\delta_M''}h(t),\qquad 0\le t\le 1. \tag{2.18}$$

Let M and N be two positive integers to generate an algorithm of space marching scheme, and then $h=\Delta x=1/M$ and $k=\Delta t=1/N$ be the parameters of the finite differences discretization of $I=[0,1]$ and $M^*=[x^*/h]$. Firstly, introducing $U_{i,n}$, $W_{i,n}$, $Q_{i,n}$, $F_{i,n}$, $Z_{i,n}$ and $E_{i,n}$ as discrete computed approximations of (respectively) $v(ih,nk)$, $v_t(ih,nk)$, $v_x(ih,nk)$, $f(ih,nk)$, $Zeta(nk)$ and $Eta(nk)$ and then the algorithm regarding solving the problem (2.13)-(2.16) may be written as follows

(1) Select δ_0, δ_0^* and δ'.

(2) Perform mollification of φ_1^ε,φ_2^ε in the interval $[0,1]$.
$U_{M^*,n}=J_{\delta_{M^*}}\varphi_1^\varepsilon(nk)\ (n\neq 0)$, $\quad U_{i,0}=J_{\delta_i'}f^\varepsilon(ih)$, $i\in\{0,1,\dots,M\}$,
$Q_{M^*,n}=J_{\delta_{M^*}^*}\varphi_2^\varepsilon(nk)$.

(3) Perform mollified differentiation in time of $J_{\delta_{M^*}}\alpha^\varepsilon(nk)$. Set
$W_{M^*,n}=\mathbf{D}_t(J_{\delta_{M^*}}\varphi_1^\varepsilon(nk))\ (n\neq 0)$, $\quad W_{M^*,0}=\mathbf{D}_t(J_{\delta_{M^*}'}f^\varepsilon(M^*h))$.

(4) Initialize $i=M^*$. Do while $i\le M-1$,

$$U_{i+1,n} = U_{i,n}+hQ_{i,n},\ (n\neq 0), \tag{2.19}$$

$$Q_{i+1,n} = Q_{i,n}+\frac{h}{a^2}\left(W_{i,n}-F_{i,n}\right), \tag{2.20}$$

$$W_{i+1,n} = W_{i,n}+h\,\mathbf{D}_t(J_{\delta_i^*}Q_{i,n}). \tag{2.21}$$

(5) Initialize $i=M^*$. Do while $i\ge 1$,

$$U_{i-1,n} = U_{i,n}-hQ_{i,n},\ (n\neq 0), \tag{2.22}$$

$$Q_{i-1,n} = Q_{i,n}-\frac{h}{a^2}\left(W_{i,n}-F_{i,n}\right), \tag{2.23}$$

$$W_{i-1,n} = W_{i,n}-h\,\mathbf{D}_t(J_{\delta_i^*}Q_{i,n}). \tag{2.24}$$

Finally

$$Z_n = \frac{1}{U_{0,n}}\left[J_{\delta_0''}g(t) - Q_{0,n}\right], \tag{2.25}$$

$$E_n = \frac{1}{U_{M,n}}\left[J_{\delta_M''}h(t) - Q_{M,n}\right]. \tag{2.26}$$

From now on, to simplify the notations, it is denoted $|X_i| = \max_n |X_{i,n}|$ if $X_{i,n}$ is a discrete function. In addition, a smoothing assumption is considered to discuss the stability and convergence of the scheme as follows

$$u(x,t) \in C^2(I \times I).$$

3. Stability and convergence analysis

In this section, the stability and convergence of the proposed marching scheme are analyzed.

Theorem 3.1 (Stability of the algorithm)**.** *For the forward algorithm* (2.19)-(2.21) *there exists a constant* Λ_1 *such that*

$$\Lambda_1 \max\{|U_M|, |Q_M|, |W_M|, M_f\} \leq \max\{|U_{M^*}|, |Q_{M^*}|, |W_{M^*}|, M_f\},$$

and for the backward algorithm (2.22)-(2.24) *there exists a constant* Λ_2 *such that*

$$\Lambda_2 \max\{|U_0|, |Q_0|, |W_0|, M_f\} \leq \max\{|U_{M^*}|, |Q_{M^*}|, |W_{M^*}|, M_f\}.$$

Proof. Firstly, the first inequality is proved.

Considering $|\delta|_{-\infty} = \min_i(\delta_i, \delta_i^*, \delta_i')$ and $M_f = \max_{(x,t)\in[0,1]\times[0,1]}\{|f(x,t)\}$ and applying theorem 2.4 from [6] yields

$$|\mathbf{D}_t(Q_{i,n})| \leq \frac{C}{|\delta|_{-\infty}}|Q_{i,n}|, \tag{3.1}$$

where C is a constant. Now as a result of using (2.21) and (3.1)

$$|W_{i+1,n}| \leq \left(1 + h\frac{C}{|\delta|_{-\infty}}\right)\max\{|Q_{i,n}|, |W_{i,n}|\}. \tag{3.2}$$

Besides, from (2.19) and (2.20) we have

$$|U_{i+1,n}| \leq (1+h)\max\{|U_{i,n}|, |Q_{i,n}|\}, \tag{3.3}$$

$$|Q_{i+1,n}| \leq \left(1 + \frac{h}{a^2}\right)\max\{|Q_{i,n}|, |W_{i,n}|, M_f\}. \tag{3.4}$$

Let $C_\delta = \max\left\{1, \frac{1}{a^2}, \frac{C}{|\delta|_{-\infty}}\right\}$, it can be obtained from (3.2)-(3.4)

$$\max\{|U_{i+1}|, |Q_{i+1}|, |W_{i+1}|, M_f\} \leq (1 + hC_\delta) \max\{|U_i|, |Q_i|, |W_i|, M_f\},$$

and then, iterating the last inequality $M_1 = M - M^*$ times leads to the following equation

$$\max\{|U_M|, |Q_M|, |W_M|, M_f\} \leq (1 + hC_\delta)^{M_1} \max\{|U_{M^*}|, |Q_{M^*}|, |W_{M^*}|, M_f\},$$

which implies

$$\max\{|U_M|, |Q_M|, |W_M|, M_f\} \leq \exp(C_\delta) \max\{|U_{M^*}|, |Q_{M^*}|, |W_{M^*}|, M_f\}.$$

The first inequality is proved with assumption $\Lambda_1 = \exp(C_\delta)$. Now it is time to prove the second inequality. Similarly, from(2.22)-(3.1)

$$|U_{i-1,n}| \leq (1 + h) \max\{|U_{i,n}|, |Q_{i,n}|\}, \tag{3.5}$$

$$|Q_{i-1,n}| \leq \left(1 + \frac{h}{a^2}\right) \max\{|Q_{i,n}|, |W_{i,n}|, M_f\}, \tag{3.6}$$

$$|W_{i-1,n}| \leq \left(1 + h\frac{C}{|\delta|_{-\infty}}\right) \max\{|Q_{i,n}|, |W_{i,n}|\}. \tag{3.7}$$

Letting $C_\delta = \max\left\{1, \frac{1}{a^2}, \frac{C}{|\delta|_{-\infty}}\right\}$ and using (3.8)-(3.10)

$$\max\{|U_{i-1}|, |Q_{i-1}|, |W_{i-1}|, M_f\} \leq (1 + hC_\delta) \max\{|U_i|, |Q_i|, |W_i|, M_f\},$$

Iterating this inequality M^* times leads

$$\max\{|U_0|, |Q_0|, |W_0|, M_f\} \leq (1+hC'_\delta)^{M^*} \max\{|U_{M^*}|, |Q_{M^*}|, |W_{M^*}|, M_f\}$$

which means

$$\max\{|U_0|, |Q_0|, |W_0|, M_f\} \leq \exp(C'_\delta) \max\{|U_{M^*}|, |Q_{M^*}|, |W_{M^*}|, M_f\}.$$

Finally with assumption $\Lambda_2 = \exp(C'_\delta)$ the second inequality is proved. □

Theorem 3.2 (Formal convergence)**.** *For fixed δ as h, k and ε tend to zero, the discrete mollified solution converges to the mollified exact solution restricted to the grid points.*

Proof. Here the convergence of the forward marching scheme (2.19)-(2.21) is going to be proved only since the convergence of the backward marching scheme (2.22)-(2.24) may be proved similarly. From the definitions of discrete error functions let

$$\Delta U_{i,n} = U_{i,n} - v(ih, nk), \quad \Delta Q_{i,n} = Q_{i,n} - v_x(ih, nk),$$
$$\Delta W_{i,n} = W_{i,n} - v_t(ih, nk).$$

Using Taylor series, a number of useful equations satisfied by the mollified solution v can be obtained, namely,

$$\begin{aligned}
v((i+1)h, nk) &= v(ih, nk) + hv_x(ih, nk) + O(h^2),\\
v_x((i+1)h, nk) &= v_x(ih, nk) + \frac{h}{a^2}\left(v_t(ih, nk) - f(ih, nk)\right) + O(h^2),\\
v_t((i+1)h, nk) &= v_t(ih, nk) + h\left(\frac{d}{dt}v_x(ih, nk)\right) + O(h^2).
\end{aligned}$$

One may write

$$\begin{aligned}
\Delta U_{i+1,n} &= \Delta U_{i,n} + (U_{i+1,n} - U_{i,n}) - (v((i+1)h, nk) - v(ih, nk))\\
&= \Delta U_{i,n} + h\Delta Q_i^n + O(h^2), \qquad (3.8)
\end{aligned}$$

$$\begin{aligned}
\Delta Q_{i+1,n} &= \Delta Q_{i,n} + (Q_{i+1,n} - Q_{i,n}) - (v_x((i+1)h, nk) - v_x(ih, nk))\\
&= \Delta Q_{i,n} + \frac{h}{a^2}\Delta W_{i,n} + O(h^2), \qquad (3.9)
\end{aligned}$$

$$\begin{aligned}
\Delta W_{i+1,n} &= \Delta W_{i,n} + (W_{i+1}^n - W_i^n) - (v_t((i+1)h, nk) - v_t(ih, nk))\\
&= \Delta W_{i,n} + h(\mathbf{D}_t(J_{\delta_i^*}Q_{i,n}) - v_{xt}(ih, nk)) + O(h^2). \qquad (3.10)
\end{aligned}$$

Now from equalities (3.8)-(3.10), using the error estimates of discrete mollification from Theorem 2.3 from [6] we have

$$\begin{aligned}
|\Delta U_{i+1,n}| &\leq |\Delta U_{i,n}| + h|\Delta Q_{i,n}| + O(h^2),\\
|\Delta Q_{i+1,n}| &\leq |\Delta Q_{i,n}| + \frac{h}{a^2}|\Delta W_{i,n}| + O(h^2),\\
|\Delta W_{i+1,n}| &\leq |\Delta W_{i,n}| + h\left(C\frac{|\Delta Q_{i,n}| + k}{|\delta|_{-\infty}} + C_{\delta^*}k^2\right) + O(h^2).
\end{aligned}$$

Suppose

$$\Delta_i = \max\{|\Delta U_{i,n}|, |\Delta W_{i,n}|, |\Delta Q_{i,n}|\},$$

$$C_0 = \max\left\{1, \frac{1}{a^2}, \frac{C}{|\delta|_{-\infty}}\right\},\ C_1 = \frac{ck}{|\delta|_{-\infty}} + C_{\delta^*}k^2.$$

Then we obtain

$$\Delta_{i+1} \leq (1 + hC_0)\Delta_i + hC_1 + O(h^2) \leq (1 + hC_0)(\Delta_i + C_1) + O(h^2),$$

and after L iterations

$$\Delta_L \leq \exp(C_0)(\Delta_0 + C_1). \qquad (3.11)$$

Moreover from

$$\begin{aligned}|\Delta U_{M^*,n}| &\leq C(\varepsilon+k),\\ |\Delta Q_{M^*,n}| &\leq C(\varepsilon+k),\\ |\Delta W_{M^*,n}| &\leq \frac{C}{\delta_{M^*}}(\varepsilon+k)+C_\delta k^2,\end{aligned}$$

It can be observed that when ε, h, and k tend to 0, Δ_0 and C_1 tend to 0. Consequently $(\Delta_0 + C_1)$ tends to 0 and so does Δ_L and this completes the proof of this theorem. □

4. Numerical examples

In this section, two numerical results are presented. In all cases, without loss of generality, we set $p = 3$ (see [7]). The radii of mollification are always chosen automatically using the mollification and GCV methods. Discretized measured approximations of boundary data are modeled by adding random errors to the exact data functions. For example, for the boundary data function $h(x,t)$, its discrete noisy version is generated by

$$h^\varepsilon_{j,n} = h(x_j,t_n) + \varepsilon_{j,n}, \qquad j = 0,1,\ldots,N, n = 0,1,\ldots,T,$$

where the$(\varepsilon_{j,n})$'s are Gaussian random variables with variance ε^2.
The errors exact and approximate solution are measured by the relative weighted l_2-norm given by

$$\frac{\left[(1/(M+1)(N+1))\Sigma_{i=0}^{M}\ \Sigma_{j=0}^{N}|v(ih,jl)-U_{i,j}|^2\right]^{1/2}}{\left[(1/(M+1)(N+1))\Sigma_{i=0}^{M}\ \Sigma_{j=0}^{N}|v(ih,jl)|^2\right]^{1/2}}.$$

Example 4.1. As the first test case, in problem (2.5)-(2.8) consider

$$x^* = 0.65,\ \varphi_1(t) = \frac{13t}{10(t^2+569/400)}+1,\ \varphi_2(t) = \frac{2t(t^2+231/400)}{(t^2+569/400)^2},\ \gamma(x)=1,$$

$$f(x,t) = \frac{2x(-t^4+24t^3-8tx^2+24t+x^4+2x^2+1)}{(t^2+x^2+1)^3},\ k(t)=\sin(t),\ h(t)=\cos(t).$$

The exact solution for $u(x,t)$ may be derived as

$$u(x,t) = \frac{(x+t)^2+1}{1+x^2+t^2},\ \zeta(t) = \sin(t) - \frac{2t}{t^2+1},\ \eta(t) = (t^2+2)\left(\cos(t) - \frac{2t^3}{(t^2+2)^2}\right).$$

Table 1 shows the comparison between the exact and numerical solutions and the relative l_2 errors. Figures 1 and 2 demonstrate the comparison between the exact and numerical results for the functions $\zeta(t)$ and $\eta(t)$ for three noise levels $\epsilon = 0.01,\ 0.001,\ 0.0001$ when $M = N = 64$

TABLE 1. Relative l_2 error norms for Example 4.1.

M	N	ε	v	v_t	v_x	ζ	η
128	128	0.0001	0.0012996	0.0085254	0.0031048	0.0053743	0.002487
256	256	0.0001	0.00094905	0.011001	0.0028282	0.0055478	0.0020288
512	512	0.0001	0.00076799	0.012082	0.0026855	0.0070051	0.0017318
1024	1024	0.0001	0.00030978	0.0046026	0.0010416	0.0035897	0.00093223
128	128	0.001	0.0012372	0.01329	0.0033996	0.0054388	0.0028889
256	256	0.001	0.000877	0.014497	0.0030274	0.0066642	0.0026709
512	512	0.001	0.00069051	0.016522	0.0031956	0.018784	0.0043266
1024	1024	0.001	0.0002675	0.024003	0.0015646	0.031533	0.006938
128	128	0.01	0.00097665	0.023496	0.0047145	0.013806	0.0055608
256	256	0.01	0.0014169	0.040586	0.0054737	0.034067	0.0088908
512	512	0.01	0.0011731	0.087198	0.004451	0.077764	0.017649
1024	1024	0.01	0.0013244	0.080186	0.0028624	0.074567	0.016956

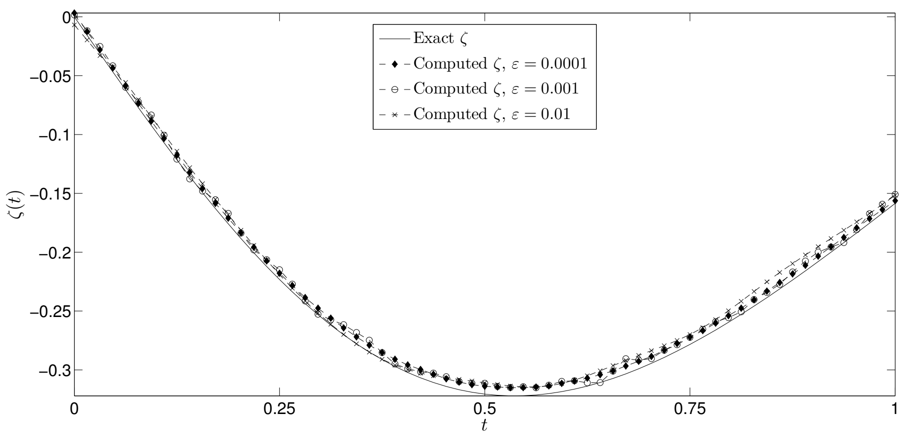

FIGURE 1. The analytical and numerical solutions for the boundary function $\zeta(t)$ for Example 4.1.

(64 was chosen since less mesh points was more visible than others in the graph). Furthermore Figures 3 and 4 show the absolute error between the exact and computed $\zeta(t)$ and $\eta(t)$ in three noise levels $\epsilon = 0.01,\ 0.001,\ 0.0001$ when $M = N = 64$

As it is expected the smaller finite difference steps, the better l_2-norm in the solutions. It can be clearly observed that there is significant difference between the solution that has been obtained from $M = N = 64$ and the one has been obtained from $M = N = 1024$. The conspicuous point in the figures is that the solutions are almost stable even with a higher level of noise.

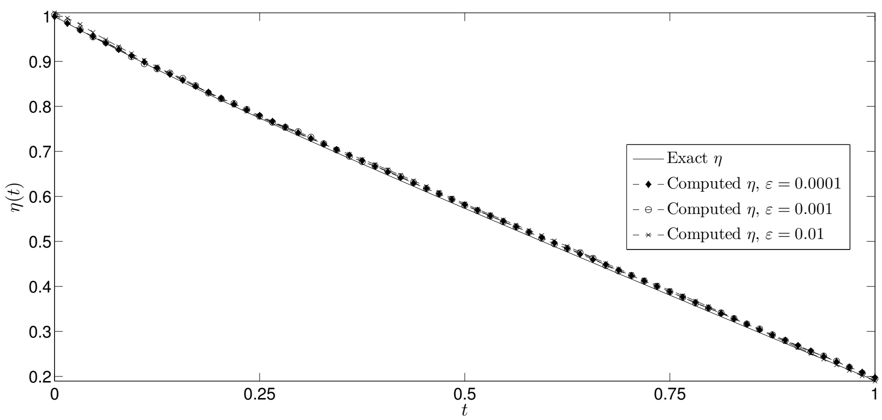

FIGURE 2. The analytical and numerical solutions for the boundary function $\eta(t)$ for Example 4.1.

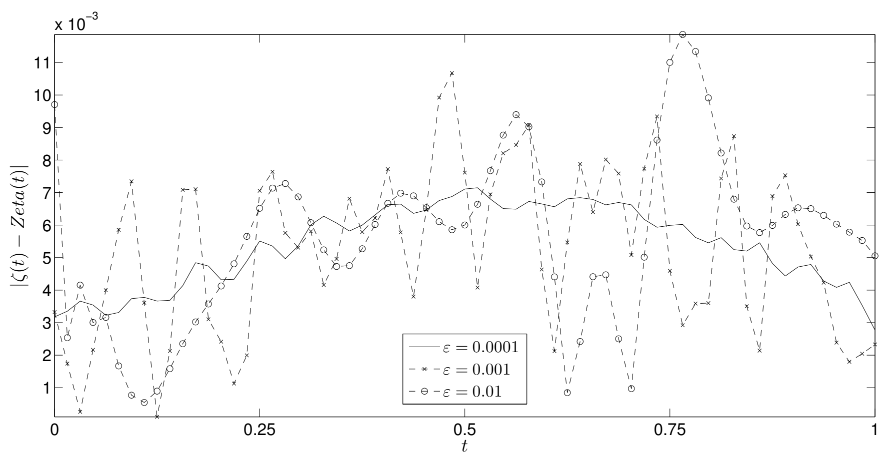

FIGURE 3. The absolute error between the exact and computed $\zeta(t)$ in three noise levels for Example 4.1 ($M = N = 64$).

Example 4.2. In the problem (2.5)-(2.8) consider

$$x^* = 0.5,\ \varphi_1(t) = 0,\ \varphi_2(t) = -\pi e^{-t},\ \gamma(x) = \cos(\pi x),$$
$$f(x,t) = 0,\ k(t) = \tanh(t) + 1,\ h(t) = \tanh(t) + 1.$$

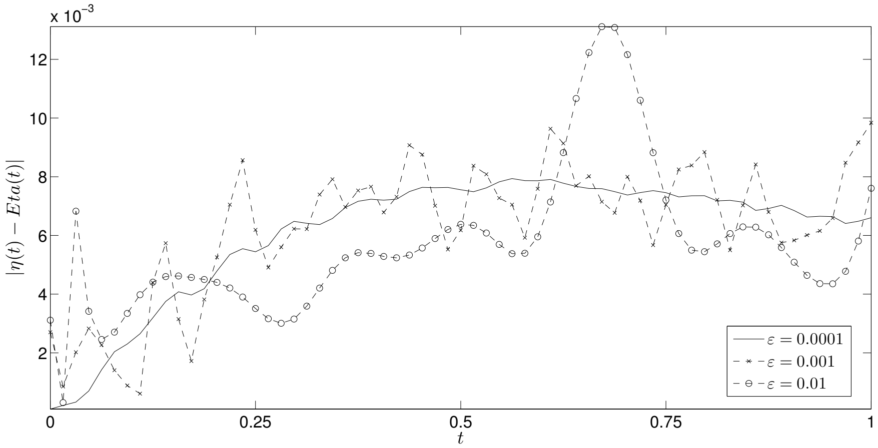

FIGURE 4. The absolute error between the exact and computed $\eta(t)$ in three noise levels for Example 4.1 ($M = N = 64$).

The exact solution for $u(x,t)$ may be derived as

$$u(x,t) = e^{-t} + \cos(\pi x),\ \zeta(t) = e^{t}(\tanh(t)+1),\ \eta(t) = -e^{t}(\tanh(t)+1).$$

Table 1 shows the comparison between the exact and numerical solutions and the relative l_2 errors. Figures 5 and 6 compare the exact and numerical results for the functions $\zeta(t)$ and $\eta(t)$ for three noise levels $\epsilon = 0.01,\ 0.001,\ 0.0001$ when $M = N = 64$. The absolute error between the exact and computed $\zeta(t)$ and $\eta(t)$ in three noise levels $\epsilon = 0.01,\ 0.001,\ 0.0001$ when $M = N = 64$ are demonstrated in the Figures 7 and 8 for three noise levels $\epsilon = 0.01,\ 0.001,\ 0.0001$ when $M = N = 64$.

TABLE 2. Relative l_2 error norms for Example 4.2.

M	N	ε	v	v_t	v_x	ζ	η
128	128	0.0001	0.011308	0.0078255	0.014317	0.037886	0.018427
256	256	0.0001	0.0057044	0.0062057	0.0071703	0.018763	0.0090689
512	512	0.0001	0.002892	0.0052849	0.0036225	0.0092635	0.0046467
1024	1024	0.0001	0.0015252	0.0081113	0.0019591	0.0052981	0.0045298
128	128	0.001	0.011564	0.020737	0.014438	0.036885	0.018829
256	256	0.001	0.0061052	0.020922	0.0075559	0.019681	0.013457
512	512	0.001	0.0033298	0.017317	0.0041267	0.010615	0.0086791
1024	1024	0.001	0.0020974	0.027872	0.0026545	0.01182	0.015628
128	128	0.01	0.012465	0.037556	0.014769	0.036638	0.020994
256	256	0.01	0.0073294	0.082729	0.0098999	0.030019	0.034128
512	512	0.01	0.0048359	0.03791	0.0045608	0.014056	0.014843
1024	1024	0.01	0.0030146	0.033548	0.0032274	0.0062359	0.0080511

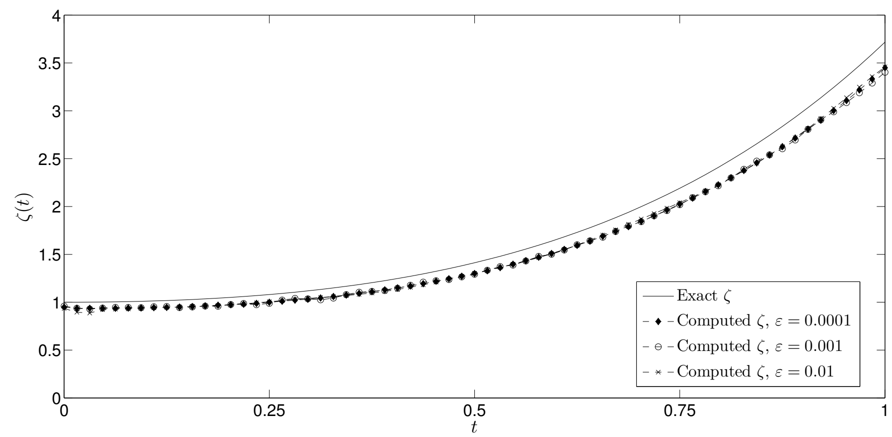

FIGURE 5. The analytical and numerical solutions for the boundary functions $\zeta(t)$ for Example 4.2.

The numerical results show a good agreement between numerical and exact solutions and more, the stability of numerical solutions with respect to the noises in input data.

5. Conclusion

As a conclusion, a class of inverse heat conduction problems has been investigated in this work. The main goal of this work was the estimation of two unknown boundary functions. To this end at an interior point, the temperature and heat flux have been considered as overspecified condition. The known initial and boundary functions have considered

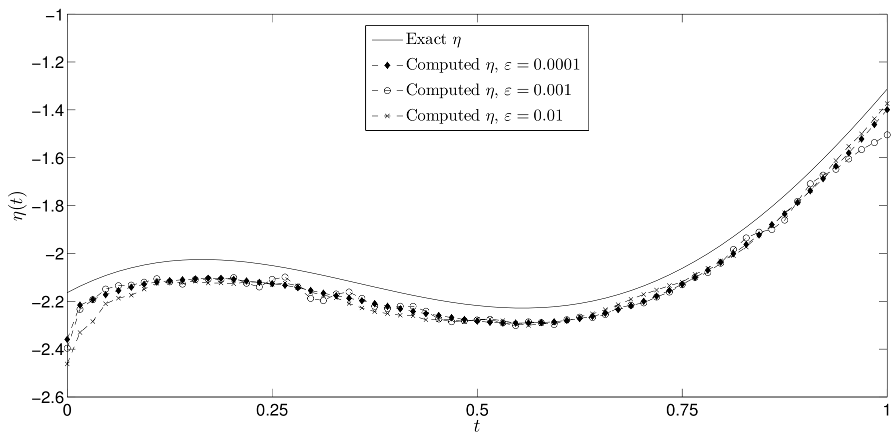

FIGURE 6. The analytical and numerical solutions for the boundary functions $\eta(t)$ for Example 4.2.

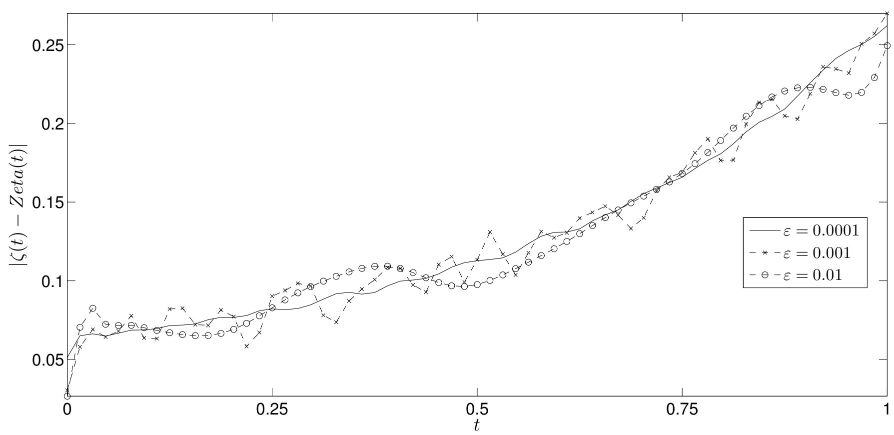

FIGURE 7. The absolute error between the exact and computed $\zeta(t)$ in three noise levels for Example 4.2 ($M = N = 64$).

noisy, and then a spatial regularization method based on mollification scheme and space marching method was applied to solve the proposed

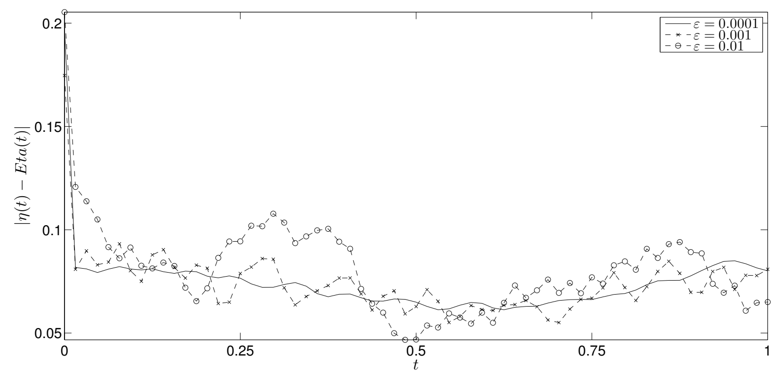

FIGURE 8. The absolute error between the exact and computed $\eta(t)$ in three noise levels for Example 4.2 ($M = N = 64$).

non-well posed inverse problem. The error analysis in this study have demonstrated the stability and convergence of the proposed method.

References

[1] B. Anderssen, F. de Hogg and M. Hegland, *A stable finite difference ansatz for higher order differentiation of nonexact data*, Bull. Austral. Math. Soc., **58** (1998), 223–232.

[2] C. Coles and D.A. Murio, *Simultaneous space diffusivity and source term reconstruction in 2D IHCP*, Computers Math. Applic., **12** (2001), 1549–1564.

[3] J.R. Cannon , *The One-Dimensional Heat Equation*, New York: Addison-Wesley (1984).

[4] Z.C. Deng, L. Yang , J.N. Yu, *Identifying the radiative coefficient of heat conduction equations from discrete measurement data*, Appl. Math.Lett., **22** (2009), 495-500.

[5] M. Garshasbi and J. Damirchi and P. Reihani, *Parameter estimation in an inverse initial boundary value problem of heat equation*, Journal of Advanced Research in Differential Equations, **2** (2010), 1943–0248.

[6] M. Garshasbi and P. Reihani and H. Dastour, *A stable numerical solution of a class of semi-linear Cauchy problems*, J. Adv. Res. Dyn. Cont. Sys. **4** (2012), 56–67.

[7] A. Hasanov, *Simultaneous determination of source terms in a linear parabolic problem from the final overdetermination: weak solution approach*, J. Math. Anal. Appl., **330** (2007), 766-779.

[8] T. Johansson, D. Lesnic, *Determination of a spacewise dependent heat source*, J. Comput. Appl. Math., **209** (2007), 66-80.

[9] Y.L. Keung, J. Zou, *Numerical identifications of parameters in parabolic systems*, Inverse Problems, **14** (1998), 83-100.
[10] D.A. Murio, *Stable numerical solution of a fractional-diffusion inverse heat conduction problem*, Computers Math. Applic., **53** (2007), 1492–1501.
[11] D.A. Murio, *Mollification and Space Marching*, Woodbury K. ,Inverse Engineering Handbook, CRC Press: Boca Raton (2002), 226–332.
[12] D.A. Murio, *The Mollification Method and the Numerical Solution of Ill-Posed Problems*, New York: John Wiley and Sons (1993).
[13] D.A. Murio and ZH. Yi, *Source Term Identification in 1-D IHCP*, Computers Math. Applic., **47** (2004), 1921–1933.
[14] M. Necati Ozisik, *Heat conduction*, New York: John Wiley & Sons (1993).
[15] L. Yang, J.N. Yu, Z.C. Deng, *An inverse problem of identifying the coefficient of parabolic equation*, Appl. Math. Model., **32** (2008), 1984-1995.

Morteza Garshasbi
School of Mathematics, Iran University of Science and Technology, Tehran, Iran
Email: `m_garshasbi@iust.ac.ir`

Hatef Dastour
School of Mathematics, Iran University of Science and Technology, Tehran, Iran
Email: `hatefdastour@gmail.com`